Ferri, J.; Garcia-Garcia, D.; Carbonell-Verdu, A.; Fenollar, O.; Balart, R. (2018). Poly(lactic acid) formulations with improved toughness by physical blending with thermoplastic starch. Journal of Applied Polymer Science. 135(4). doi:10.1002/app.45751

"Poly(lactic acid) formulations with improved toughness by physical blending with thermoplastic starch"

J.M. Ferri, D. Garcia-Garcia, A. Carbonell-Verdú, O. Fenollar, R. Balart

Instituto de Tecnología de Materiales (ITM)
Universitat Politècnica de València (UPV)
Plaza Ferrándiz y Carbonell s/n, 03801, Alcoy, Alicante, Spain
Corresponding author: joferaz@upvnet.upv.es

Abstract

This work focuses on poly(lactic acid) (PLA) formulations with improved toughness by physical blending with thermoplastic maize starch (TPS) plasticized with aliphatic-aromatic copolyester (AAPE) up to 30 wt%. A noticeable increase in toughness is observed, due to the finely dispersed spherical TPS domains in the PLA matrix. It is worth to note the remarkable increase in the elongation at break that changes from 7% (neat PLA) up to 21.5% for PLA with 30 wt% TPS. The impact-absorbed energy is markedly improved from the relatively low values of neat PLA (1.6 J m^{-2}) up to more than three times. Although TPS is less thermally stable than PLA due to its plasticizer content, in general, PLA/TPS blends offer good balanced thermal stability. The morphology reveals high immiscibility in PLA/TPS blends, with TPS-rich domains with an average size of 1 μm, finely dispersed which, in turn, is responsible for the improved toughness.

1. Introduction.

The packaging industry is facing an important challenge, which is the increasing use of environmentally friendly materials to avoid waste generation. For this reason, the use of biodegradable (disintegrable in controlled compost conditions) polymers is continuously growing. Biodegradable polymers include some petroleum-based polyesters such as poly(caprolactone) (PCL) [1], poly(butylene succinate) (PBS) [2], poly(butylene succinate–*co*–adipate) (PBSA) [3], poly(butylene adipate-co-terephthalate) (PBAT) [4], etc, among others. In addition, some biodegradable polymers can be obtained from renewable resources as it is the case of poly(lactic acid) (PLA) [5], bacterial polyesters such as poly(hydroxybutyrate) (PHB)[6], poly(hydroxybutyrate-*co*-valerate) (PHBV)[7], protein-based polymers (gluten, casein, soy protein, etc.), and polysaccharide polymers (chitosan, cellulose, starch, etc.).

PLA offers good perspectives at present and in the near future for use in the packaging industry [8-11]. Its possesses good mechanical properties, together with balanced barrier properties; in addition, it can be disintegrated in soil compost [12]. All these features, along with its increasingly competitive price, have led PLA to an advantageous position against other biodegradable polymers. PLA can be obtained from starch-rich materials such as some cereals (wheat, corn) and some roods (beetroot, cassava, yucca, etc.) [13, 14]. However, not all are advantages; some of its disadvantages are related to its low elongation at break, low flexibility and toughness. To overcome these drawbacks, different strategies have been proposed. Copolymerization is highly interesting from a technical standpoint but it is not a cost-effective solution. Plasticization is a cost-effective approach but it is important to take into account the plasticizer migration. However, many plasticizers of natural origin are permitted for use in packaging, such as those normally used in formulations of TPS. Physical blending with ductile and flexible polymers is an interesting solution but there are some issues related with the miscibility between the components that must be addressed to obtain optimum properties. Blending with thermoplastic starch (TPS) is a cost-effective solution as it can provide increased flexibility, elongation at break and, subsequently, a marked improvement on toughness can be achieved [13, 15]. Therefore, TPS is a plasticized polymer and obtained from starch-rich plants or foods such as pea, corn, sorghum, barley, amaranth, yucca, sweet potato, etc. [16], etc. Industrial formulations of TPS need certain amounts of a plasticizer such as water [17, 18], glycerol, sorbitol, xylitol, glucose or combinations [19, 20] to improve ductility,

cohesion, elongation at break and resistance to retrogradation as well as to increase the overall thermal stability [21, 22]. Starch is chemically constituted of two types of polysaccharides: amylose and amylopectin and, in a less extent, some lipids. Depending on the origin, the amylose/amylopectin ratio varies and this has a direct influence on mechanical properties [23-25]. Furthermore, the degree of crystallinity of starch can vary in the 15-45% range as a consequence of the abovementioned ratio and may change in time due to retrogradation phenomena [22]. The plasticizer type and content can also influence the degree of crystallinity of starch in industrial TPS formulations [21]. TPS is poorly miscible with polyhydroxyacids as it is the case of PLA [26, 27]. For this reason, new starch plasticizers are being investigated to allow somewhat interactions with other polymers.

This work explores the potential of a thermoplastic starch, plasticized with a biodegradable aliphatic/aromatic copolyester (AAPE), to obtain high toughness PLA formulations by physical blending [28]. The effect of TPS content (0 – 30 wt%) in PLA/TPS blends is evaluated in terms of mechanical and thermal properties as well as morphology.

2. Experimental.

2.1. Materials.

A commercial PLA grade Ingeo™ Biopolymer 6201D was obtained in pellet form from NatureWorks LLC (Minnetonka, USA). This PLA grade contains 2% D-lactic acid and possesses a density of 1.24 g cm^{-3} at 23 ºC and a melt flow index comprised in the 15-20 g/(10 min) range at 210 ºC. A TPS grade Mater-Bi® NF 866 was supplied by Novamont (Novara, Italy). This TPS is obtained from maize starch and is characterized by a melt flow index of 3.5 g/(10 min) at 150 ºC and a density of 1.27 g cm^{-3} at 23 ºC. Its melting peak temperature is comprised between 110 – 120 ºC and contains more than 50% of AAPE [28]. With regard to the base starch, it is composed of 73% amylopectin and 23% amylose.

2.2. Preparation of PLA/TPS blends.

The TPS content in PLA/TPS varied in the range 0 – 30 wt% as summarized in Table 1. Initially all materials were dried at 60 ºC for 24 h, weighed in the appropriate proportions and mechanically pre-mixed in a zipper bag. Then, the materials were compounded in a twin-screw co-rotating extruder from Dupra (Castalla, Spain) at 60 rpm. The temperature profile was set to 165 ºC (feeding), 170 ºC, 172.5 ºC y 175 ºC (die). After cooling, the compounded materials were pelletized and subsequently processed by injection moulding in a Meteor 270/75 from Mateu&Solé (Barcelona, Spain) at an injection temperature of 175 ºC.

Table 1. Summary of compositions and labelling of PLA/TPS formulations.

Code	PLA (wt%)	TPS (wt%)
TPS	-	100
PLA	-	100
PLA /7.5TPS	92.5	7.5
PLA /15TPS	85	15
PLA /22.5TPS	77.5	22.5
PLA /30TPS	70	30

2.3. Mechanical characterization of PLA/TPS blends.

Tensile and flexural tests were carried out in a universal testing machine ELIB 30 from S.A.E. Ibertest (Madrid, Spain) at room temperature according to ISO 527-5 and ISO 178 respectively at a crosshead speed of 10 mm min^{-1}. At least, five different samples were tested and average values of tensile strength (σ), modulus (E) and elongation at break (ε_b) were calculated. Moreover, an axial extensometer (SAE Ibertest model IB/MFQ-R2, Madrid, Spain) was used to obtain the Young's modulus in a more accurate way. Hardness measurements were obtained in a Shore D durometer model 673-D from Instrumentos J. Bot S.A. (Barcelona, Spain) following ISO 868. Impact-absorbed energy was obtained in a Charpy's pendulum from Metrotec S.A. (San Sebastián, Spain) with an energy of 1 J, as indicated in ISO 179:1993. Five different notched (notch type A) samples were tested and average values were calculated. The notch was done in a notch machine from HOYTOM S.L.(Leioa, Bizkaia, Spain) with a background radius of 0.25±0.05, a remaining width of 8.0±0.2 and a notch angle of 45º± 1º.

Dynamic mechanical thermal characterization (DMTA) was carried out using an oscillatory rheometer AR G2 from TA Instruments (New Castle, USA) equipped with a special clamp system to test solid samples in a torsion/shear mode. The samples sized 40x10x4 mm^3 and were subjected to a heating program from -80 ^oC up to 130 ^oC at a constant heating rate of 2 $^oC\ min^{-1}$. The selected frequency was 1 Hz and the maximum shear deformation percentage (%γ) was set to 0.1%.

2.4. Morphology characterization by FESEM.

A field emission scanning electron microscope (FESEM) model ZEISS ULTRA55 from Oxford Instruments (Abingdon, United Kingdom) was used to characterize the morphology of the fractured surfaces from impact tests. The acceleration voltage was set to 2 kV. Prior to observation by FESEM, all surfaces were covered with an ultrathin platinum layer by a high vacuum sputtering process in a EM MED020 sputter coater from Leica Microsystems (Wetzlar, Germany).

2.5.- Thermal characterization.

A thermogravimetric balance TGA/SDTA 851 from Mettler Toledo Inc. (Schwerzenbach, Switzerland) was used to characterize the thermal degradation of PLA/TPS blends. A dynamic program from 30 ^oC to 500 ^oC at 20 $^oC\ min^{-1}$ in nitrogen atmosphere (66 mL min^{-1}) was used. The main thermal transitions of the PLA/TPS system were studied by differential scanning calorimetry (DSC) in a Mettler-Toledo 821 calorimeter using a dynamic heating program from 30 ^oC to 350 ^oC at a heating rate of 10 $^oC\ min^{-1}$ in nitrogen atmosphere (66 mL min^{-1}).

3. Results and discussion.

3.1. Influence of TPS content on mechanical properties of PLA/TPS blends.

Fig. 1 and Fig. 2 show the evolution of tensile and flexural properties of the PLA/TPS system as a function of the TPS content. Neat PLA possesses a tensile strength of 64 MPa. This decreases almost linearly down to values of 41.5 MPa for the

PLA/TPS blend containing 30 wt% TPS. In a similar way, tensile modulus also offers a decreasing tendency with increasing TPS content. The initial tensile modulus of neat PLA is close to 3.6 GPa and decreases down to values of about 2.5 GPa (PLA/TPS blend with 30 wt% TPS). This phenomenon is typical of plasticized PLA formulations. Silverajah *et al.* reported that 5 wt% EPO plasticizer in PLA formulations led to lower tensile strength values by 26.3% with regard to neat PLA. Moreover, they reported a decrease in Young's modulus of EPO-plasticized PLA of 7% by adding 5 wt% EPO [29]. Despite this decrease in mechanical resistant properties for PLA/TPS blends with high TPS content, both tensile strength and modulus are still superior to most commodity plastics. With regard to the ductile properties, TPS has a very positive effect. Whilst PLA is characterized by a very low elongation at break value of about 7%, the addition of TPS raises this up to values of 18% and 21.5% for PLA/TPS blends containing 22.5 wt% and 30 wt% TPS, respectively. It seems to be a threshold in the range 15-22.5 wt% TPS. It is clearly observed that the elongation at break does not increase in a marked way below this threshold whilst a noticeable rise is detected over this threshold value. This could be related to the plasticizer content in TPS with a clear effect above this threshold point. It has been reported a similar effect by using PCL with an increase in elongation at break of 85% in PLA/PCL blends with 22.5 wt% PCL [30]. Nevertheless, TPS is a more cost-effective solution to PCL due to its lower cost compared to PCL and other polyester polymers. In a first approach, TPS offers restricted miscibility with PLA [26, 27]. Nevertheless, the results herein shown, indicate a synergistic effect that could be related with the particular plasticizer in TPS as it is a copolyester-type that could interact with the polyester structure of PLA chains. AAPE contains aromatic groups that make this plasticizer increase the solubility between the commercial TPS and the PLA, showing benefits in the ductile properties.

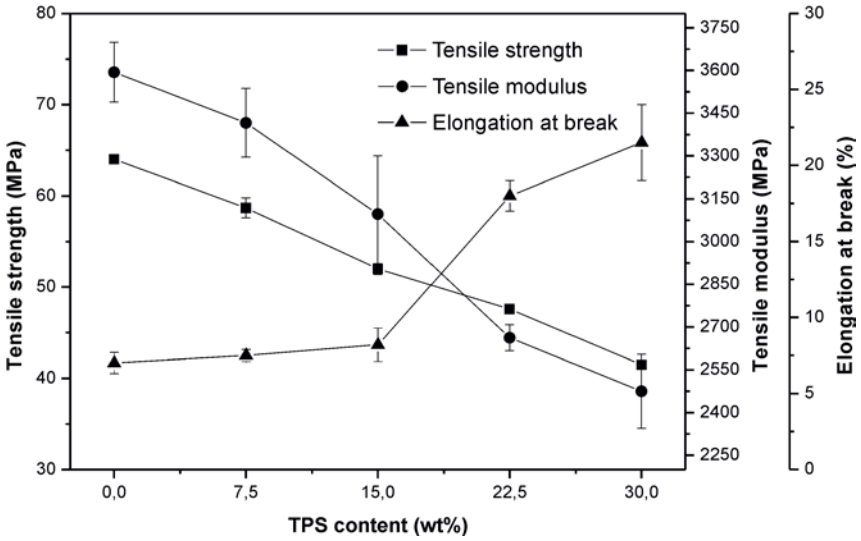

Figure 1. Plot evolution of mechanical properties from tensile tests as a function of the weight % TPS.

Similar tendency can be observed for flexural properties (Fig. 2). The flexural strength and modulus of neat PLA, 116.3 MPa and 3.27 GPa, respectively, decrease down to values of 64.8 MPa and 2.24 GPa respectively in the PLA/TPS blend with 30 wt% TPS. Although the plasticizing effect of TPS is not so pronounced as is discussed in the thermal analysis section, the effects on mechanical properties are quite similar and this could be related to the particular structure of this biphasic polymer system with a fragile matrix of PLA in which, spherical particles of a very flexible polymer (TPS) are finely dispersed.

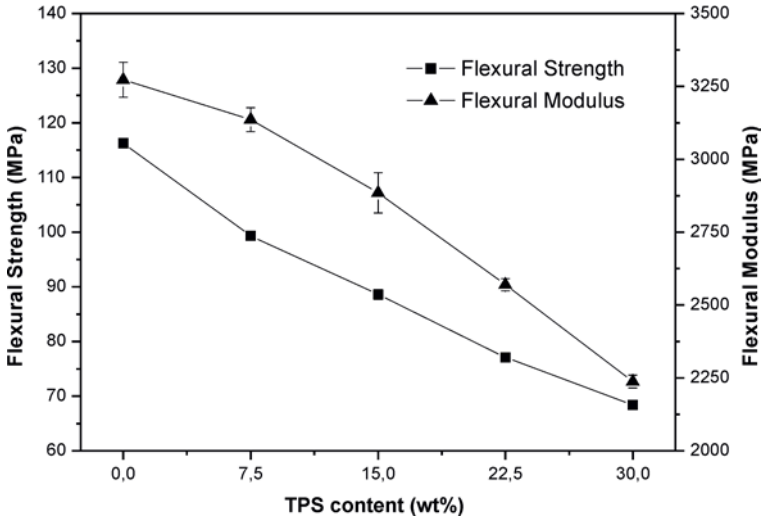

Figure 2. Plot evolution of flexural strength and flexural modulus from PLA/TPS blends as a function of the weight % TPS.

As expected, as the TPS content increases, Shore D hardness values are lower as observed in Table 2.

Table 2. Impact-absorbed energy, Shore D hardness and thermomechanical properties of PLA/TPS blends as a function of the weight % TPS.

wt% TPS	Charpy's impact-absorbed energy (kJ m^{-2})	Shore D hardness	Vicat softening temperature, VST (°C)	Heat deflection temperature, HDT (°C)
0	1.6 ± 0.3	76.0 ± 0.5	52.8 ± 1.4	47.6 ± 1.0
7.5	1.9 ± 0.3	73.8 ± 0.3	52.6 ± 1.2	49.2 ± 1.2
15	2.8 ± 0.3	72.5 ± 0.7	52.4 ± 0.6	49.0 ± 0.8
22.5	3.7 ± 0.1	69.9 ± 0.9	51.4 ± 0.8	49.2 ± 1.0
30	5.3 ± 0.1	68.2 ± 0.6	50.6 ± 1.0	49.4 ± 0.8

It is worthy to note the positive effect of TPS on PLA/TPS blends toughness. Neat PLA is characterized by an extremely low toughness, directly related to its intrinsic fragility. As we have described previously, addition of TPS to PLA, leads to decreased mechanical resistant properties and a marked increase in the elongation at break which is directly related to the ability of the material to absorb energy. For this reason, the impact-absorbed energy change from 1.6 kJ m^{-2} (neat PLA) up to more than 3 times higher values of 5.3 kJ m^{-2} for PLA/TPS blends with 30 wt% TPS. Once again, although it is not expected a high miscibility between PLA and TPS, it is possible that the particular biphasic structure of the PLA/TPS systems contributes to improved toughness. Ojijo *et al.* observed a high increase in toughness of PLA by blending with poly(butylene succinate-co-adipate)(PBSA). Adding 30 wt% of PBSA, the absorption of energy to the impact increased 21.4%. Regarding thermomechanical properties, VST and HDT values do not change in a marked way and no clear tendency can be detected since the standard deviation is within the typical variation range.

3.2. Effect of TPS content on thermal properties of PLA/TPS blends.

Fig. 3 shows a comparative plot of the DSC curves of neat PLA, TPS and their blends. Regarding neat PLA, its glass transition temperature (T_g) is close to 60 °C and is

clearly detectable by a change in slope. The exothermic peak comprised between 90 – 110 ºC is related to the cold crystallization process and, finally, the endothermic peak between 150 - 180 ºC corresponds to the melting process. The small exothermic peak that appears during heating and just before the melting peak is due to the re-crystallization of PLA [31]. At temperatures close to the melting temperature (150°), the spherulites or crystalline zones (alpha prime form) of the PLA generated at temperatures close to 100 ° C, are disordered. Then, the chains of the PLA are ordered (re-crystallized) to alpha form (more stable form)(representing an exothermic peak in Figure 3), although during this re-crystallization process and because the movement of the chains is so high, the chains quickly return to disordered giving rise to the melting process (representing an endothermic peak in Figure 3). TPS addition has a slight effect on the glass transition temperature thus showing a poor plasticization effect. The T_g of PLA is 65.4 ºC and it is decreased by 3 ºC whatever the TPS content as it can be seen in Table 3, which gathers the main thermal transitions and parameters of PLA and its blends with TPS. This slight decrease in T_g is representative for poor miscibility between PLA and TPS [26, 27]. This poor plasticization effect is also assessed by the slight decrease in the cold crystallization peak which changes from 102 ºC for neat PLA down to 98 - 99 ºC for almost all PLA/TPS blends. This low decrease in the cold crystallization peak could be related to the nucleating effect of TPS [26]. López-Rodriguez et al. reported a decrease of almost 20 ºC by the addition of 40 wt% of PCL. On the other hand, PLA plasticized by oligomeric plasticizers revealed a decrease in T_c in a range 10 to 15ºC.

Table 3. Summary of the main thermal transitions and parameters of PLA/TPS blends obtained by DSC.

wt% TPS	T_g (ºC)	T_c (ºC)	ΔH_c (J g^{-1})	T_m (ºC)	ΔH_m (J g^{-1})	%X
0	65.4	102	26.71	168.3	40.19	14.5
7.5	62.4	98.7	16.53	170.4	36.31	23.0
15	62.1	99.0	15.42	170.4	30.51	19.1
22.5	61.5	98.6	16.47	170.1	27.92	15.9
30	62.8	98.5	16.64	170.3	26.25	14.7

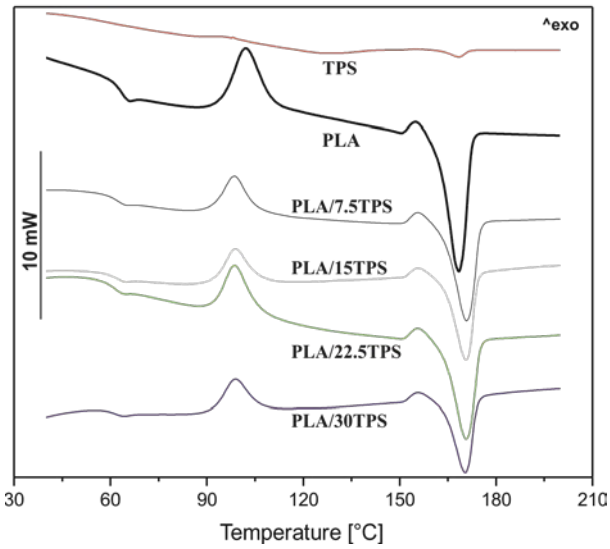

Figure 3. Comparative DSC thermograms of neat PLA, TPS and PLA/TPS blends with different weight % TPS.

With regard to the degree of crystallinity (%X) of the PLA-rich domain, low TPS addition provides elevated %X values of almost 23% which is noticeably higher than that observed for neat PLA (14.5%). Nevertheless, this effect is lost as the TPS content increases to 30 wt% TPS thus leading to similar crystallinity to neat PLA. Similar behavior has been reported by Shin BY *et al.* [32]. Adding 20% of modified TPS to PLLA 2002D, the %X increased from 0.2% to 24%. TPS acts as a nucleating agent for the crystallization of PLA. For low TPS contents (7.5%) increases the effective contact surface (The TPS are distributed in small domains and the specific area is higher than when the TPS content is higher) between the PLA and the TPS therefore increases the degree of crystallinity of the PLA. As the TPS content increases, the area in contact of the TPS domains with the PLA matrix is lower and therefore, although the TPS acts as a nucleating agent, the specific nucleation area is lower and the crystallinity is lower, but in all cases, higher than virgin PLA."

With regard to the thermal stability at high temperatures, Fig. 4 shows a comparative plot of the TGA curves of neat PLA and TPS and their corresponding blends. PLA degrades in a single step process with onset degradation temperature of 310 ºC. Regarding TPS, its degradation process occurs in two main stages. The first one occurs in the 300 – 360 ºC range with a weight loss of about 29%; this degradation stage could be attributed to the starch pyrolysis [33]. The second stage is comprised between

360 – 500 ºC with a weight loss of 61% which is related to the decomposition of the biodegradable copolyester component in TPS [34].

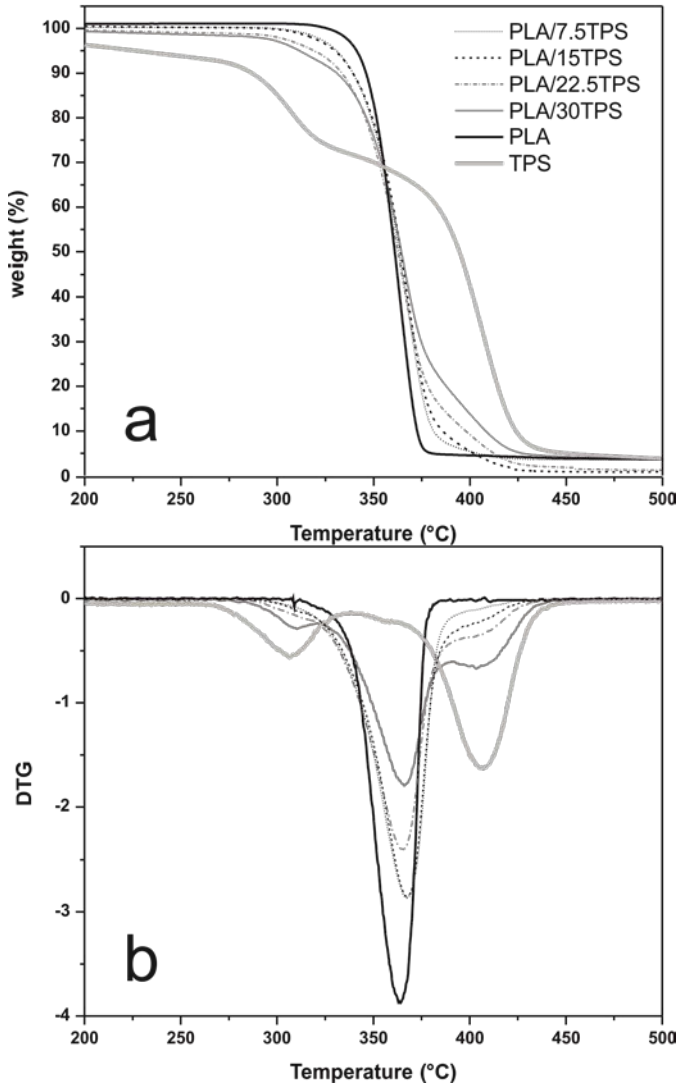

Figure 4. a) Thermogravimetric (TG) and b) derivative thermogravimetric curves (DTG) of neat PLA, TPS and their blends with different TPS content.

Table 4 shows some parameters related to the thermal degradation. In particular, the temperature at which a 5% and 90% weight loss occurs ($T_{5\%}$, $T_{90\%}$) and the maximum degradation rate temperature (T_{max}), are summarized. Although slight decrease in $T_{5\%}$ can be detected, in general, the thermal stability is not highly affected by presence of TPS. In fact, as we can observe, a slight increase in $T_{90\%}$ is detected but in both cases, the change is not significative.

Table 4. Thermal parameters of unplasticized PLA and PLA/TPS blends with various TPS content.

wt% TPS	TGA		
	$T_{5\%}$ (ºC)	$T_{90\%}$ (ºC)	T_{max} (ºC)
0	336.9	365.1	363.5
7.5	330.7	381.1	365.0
15	329.9	385.8	364.5
22.5	319.0	397.7	364.6
30	311.5	427.2	365.1

3.4. Effect of TPS content on dynamic-mechanical thermal behaviour of PLA/TPS blends.

Fig. 5 shows the evolution of the storage modulus (G') as a function of increasing temperature for both neat materials, PLA and TPS and their corresponding blends. As the TPS content increase, the characteristic G' curve moves to lower G' values. This also corroborates more flexible materials as previously described in the mechanical characterization. As it can be seen for neat PLA, G' suffers a noticeable decrease in the temperature range comprised between 55 – 70 ºC (more than two fold). This is directly related to its glass transition relaxation (T_g). If we compare the G' values at 25 ºC, the effect of TPS become clearly evident with a marked decreasing tendency. Neat PLA shows a G' value of 1.34 GPa; addition of 7.5 wt% leads to a G' value of 1.08 GPa. G' is slightly reduced in PLA/TPS blends with 15-22.5 wt% TPS, with values in the 0.95-1.0 GPa whilst minimum values of 0.6 GPa are obtained in blends with 30 wt% TPS. The evolution of G' in the glass transition relaxation zone, also indicates poor plasticization effects as the typical curves are not highly moved to lower temperatures thus indicating a slight decrease in T_g values as observed in DSC analysis. Another important transition of neat PLA is the cold crystallization process with occurs in the 80-90 ºC range. During the cold crystallization, amorphous domains in PLA tend to rearrange in a packed structure to form crystalline zones that contribute to increase its mechanical resistance and rigidity (almost two fold higher regarding the minimum values achieved after the glass transition relaxation). As it has been

previously described in the DSC analysis, the cold crystallization process occurs at lower temperatures in PLA/TPS blends, due to the slightly increased chain mobility that TPS provides. For this reason, characteristic curves are shifted by almost 10 ºC to the left with regard to neat PLA. This is in total accordance with the results shown in the DSC analysis and it is in agreement with some other works [29, 35].

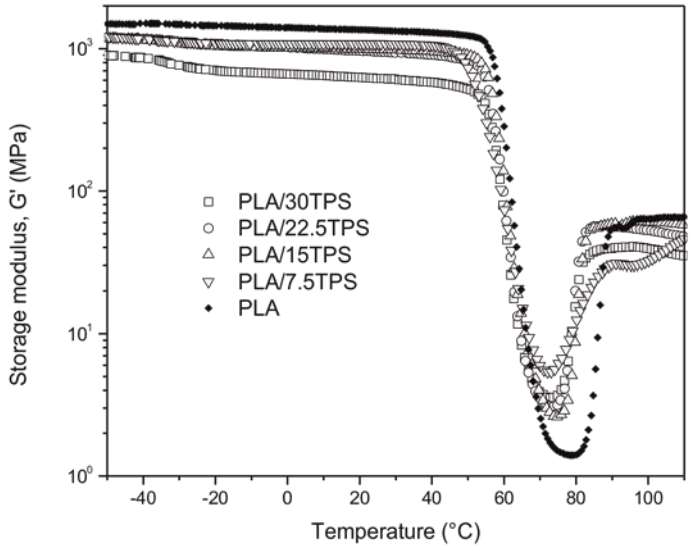

Figure 5. Plot evolution of the storage modulus (G') of neat PLA and PLA/TPS blends vs temperature for various TPS contents.

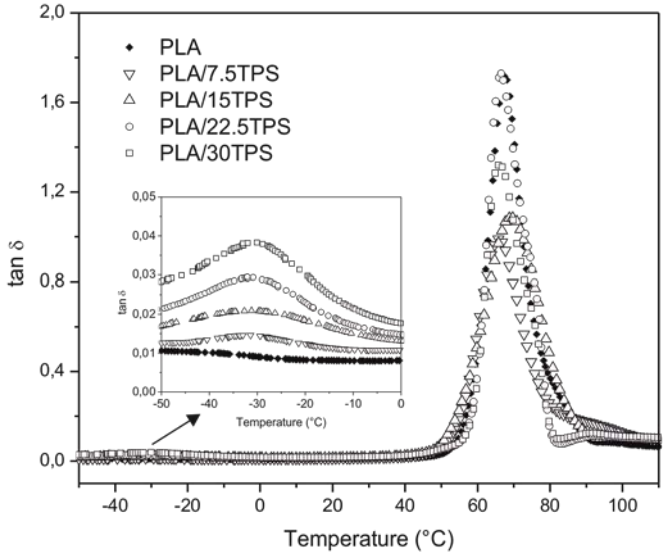

Figure 6. Plot evolution of the damping factor (tan δ) of neat PLA and PLA/TPS blends vs temperature for various TPS contents.

The change in the glass transition temperature (T_g) is more clearly detectable by analysing the evolution of the damping factor (tan δ) with temperature (Fig. 6). By

taking the damping factor peak as the criterion to estimate the T_g, neat PLA possesses a T_g value of about 68 ^oC and this is reduced by not more than 2 ^oC for PLA/TPS blends with 15-22.5 wt% TPS. This means poor plasticization effect due to restricted miscibility between these two polymers. Neat TPS shows a wide relaxation temperature range comprised between -50 ^oC and -5 ^oC with a peak (T_g) value of -28.3 ^oC as it can be seen in Fig. 6. Although the miscibility between PLA and TPS is restricted, some PLA chains enter TPS domains and contribute to slightly decrease its characteristic T_g value by 4-5 ^oC. Similarly, it occurs in the work of Ojijo et al. where they modify PBSA by adding triphenyl phosphite (TPP). In this way, the interaction between the PLA and PBSA improves significantly contributing a greater tenacity to the binary mixture.

3.5. Effect of TPS content on the morphology of PLA/TPS blends.

Fig. 7 gathers typical FESEM images of cryofractured samples of both neat PLA and TPS at different magnifications.

Figure 7

Figure 7. FESEM images of cryofractured samples of neat PLA (a and b) and TPS (c and d) at different magnifications, 1000x (a and c) and 5000x (b and d).

Figure 8

Figure 8. FESEM images of cryofractured samples of PLA/TPS blends with different TPS content: a-b) 7.5 wt%, c-d) 15.0 wt%, e-f) 22.5 wt% and g-h) 30 wt% at different magnifications, 1000x (a, c, e and g) and 5000x (b, d, f and h).

PLA (Fig. 7a and Fig. 7b) shows a typical fragile fracture surface with no evidence of plastic deformation and a homogenous smooth surface. On the other hand, TPS (Fig. 7c and Fig. 7d) shows a different fracture with flake formation typical of the growth of crystalline planes in maize starch (crystalline lamellae) which are oriented randomly during the fracture process. These planes are stacked in a parallel way due to the growth of starch A-type from the seeds. These stacked planes from small blocks

and the aggregate of blocks form granules that are separated from the amorphous zones in which, amylose and plasticizers are located [36].

Fig. 8 reveals in a clear way, the biphasic structure of the PLA/TPS system, through FESEM images of cryofractured samples. All formulations offer a biphasic structure with a PLA-rich matrix in which TPS-rich domains appear randomly dispersed. The TPS-rich domains offer different size as the TPS content increases. So that, the TPS-rich domains change from 0.2 – 0.4 μm (in PLA/TPS blends with 7.5 wt% TPS) up to 1 – 2 μm (in PLA/TPS blend with 30 wt% TPS). A similar result has been reported by Mittal V *et al.* In that work, the authors studied binary and ternary blends and showed TPS-rich domains with sizes comprised between 0.5-2 μm in a PLA/TPS blend with 50 wt% TPS. As the particle size increases we can also observe the lack (or very poor) miscibility between PLA and TPS as some spherical voids appear, thus indicating that some TPS-rich domains have been pulled out during the cryofracture process. This particular morphology, with TPS-rich domains with a size ranging from 0.2 to 2 μm, positively contributes to improved toughness as it has been described previously.

4. Conclusions.

Addition of TPS is a cost-effective method to improve the low intrinsic ductile behaviour of PLA with improved toughness. This widens its uses at industrial scale as its fragility is markedly reduced. Indeed, the elongation at break improves from 7.0% (neat PLA) up to values of 21.5% in PLA/TPS blend with 30 wt% TPS, which represents a percentage increase by more than 300%. It is worthy to note that the impact-absorbed energy is increased up to 5.3 J m^{-2} (PLA/TPS blend with 30 wt% TPS) which is more than three times the value of neat PLA (1.6 J m^{-2}). Thermal analysis has revealed a poor miscibility between PLA and TPS. In fact, DSC and DMTA revealed a reduction of 2-3 ^{o}C in T_g thus showing a restricted miscibility between these polymers. The plasticization effects that TPS can provide are restricted duo to the lack of miscibility. Nevertheless, the particular biphasic structure revealed by FESEM, with small spherical TPS-rich domains (with a size ranging between 0.2 to 2 μm) finely dispersed in the rigid PLA-rich matrix, has a positive effect on toughness and energy-absorption. As a general conclusion, blending PLA with TPS represents a cost-effective

and environmentally friendly solution to widen the uses of PLA way by improving its toughness and ductile properties.

Acknowledgements

This research was supported by the Ministry of Economy and Competitiveness - MINECO, Ref: MAT2014-59242-C2-1-R. Authors also thank to "Conselleria d'Educació, Cultura i Esport" - Generalitat Valenciana, Ref: GV/2014/008 for financial support.

References.

1. Tsuji H. and Ishizaka T. International Journal of Biological Macromolecules. 2001, *29*, 83-89.
2. Genovese L., Lotti N., Gazzano M., Siracusa V., Dalla Rosa M., and Munari A. Polymer Degradation and Stability. 2016, *132*, 191-201.
3. Ojijo V., Sinha Ray S., and Sadiku R. ACS Applied Materials & Interfaces. 2013, *5*, 4266-4276.
4. Weng Y.-X., Jin Y.-J., Meng Q.-Y., Wang L., Zhang M., and Wang Y.-Z. Polymer Testing. 2013, *32*, 918-926.
5. Balart J.F., Fombuena V., Fenollar O., Boronat T., and Sánchez-Nacher L. Composites Part B. 2016, *86*, 168-177.
6. Garcia-Garcia D., Ferri J.M., Boronat T., Lopez-Martinez J., and Balart R. Polymer Bulletin. 2016, *73*, 3333-3350.
7. Nair M.B., Baranwal G., Vijayan P., Keyan K.S., and Jayakumar R. Colloids and Surfaces B: Biointerfaces. 2015, *136*, 84-92.
8. Cheng H.-Y., Yang Y.-J., Li S.-C., Hong J.-Y., and Jang G.-W. Journal of Applied Polymer Science. 2015, *132*,
9. Ingrao C., Tricase C., Cholewa-Wojcik A., Kawecka A., Rana R., and Siracusa V. Science of the Total Environment. 2015, *537*, 385-398.
10. Jost V. and Kopitzky R. Chemical and Biochemical Engineering Quarterly. 2015, *29*, 221-246.
11. Sanyang M.L. and Sapuan S.M. Journal of food science and technology. 2015, *52*, 6445-54.
12. Plackett D.V., Holm V.K., Johansen P., Ndoni S., Nielsen P.V., Sipilainen-Malm T., Sodergard A., and Verstichel S. Packaging Technology and Science. 2006, *19*, 1-24.
13. Averous L. Journal of Macromolecular Science-Polymer Reviews. 2004, *C44*, 231-274.
14. Lasprilla A.J.R., Martinez G.A.R., Lunelli B.H., Jardini A.L., and Maciel Filho R. Biotechnology Advances. 2012, *30*, 321-328.
15. Boonprasith P., Wootthikanokkhan J., and Nimitsiriwat N. Journal of Applied Polymer Science. 2013, *130*, 1114-1123.
16. Sahari J., Sapuan S.M., Zainudin E.S., and Maleque M.A. Carbohydrate Polymers. 2013, *92*, 1711-1716.

17. Mahieu A., Terrie C., and Youssef B. Industrial Crops and Products. 2015, *72*, 192-199.
18. Chocyk D., Gladyszewska B., Ciupak A., Oniszczuk T., Moscicki L., and Rejak A. International Agrophysics. 2015, *29*, 267-273.
19. Li H. and Huneault M.A. Journal of Applied Polymer Science. 2011, *122*, 134-141.
20. Mikus P.Y., Alix S., Soulestin J., Lacrampe M.F., Krawczak P., Coqueret X., and Dole P. Carbohydrate Polymers. 2014, *114*, 450-457.
21. Schmitt H., Guidez A., Prashantha K., Soulestin J., Lacrampe M.F., and Krawczak P. Carbohydrate Polymers. 2015, *115*, 364-372.
22. Zhang Y., Rempel C., and Liu Q. Critical Reviews in Food Science and Nutrition. 2014, *54*, 1353-1370.
23. Chaudhary A.L., Miler M., Torley P.J., Sopade P.A., and Halley P.J. Carbohydrate Polymers. 2008, *74*, 907-913.
24. Chaudhary A.L., Torley P.J., Halley P.J., McCaffery N., and Chaudhary D.S. Carbohydrate Polymers. 2009, *78*, 917-925.
25. Pang M.M., Pun M.Y., and Ishak Z.A.M. Polymer Engineering and Science. 2014, *54*, 1357-1365.
26. Teixeira E.d.M., Curvelo A.A.S., Correa A.C., Marconcini J.M., Glenn G.M., and Mattoso L.H.C. Industrial Crops and Products. 2012, *37*, 61-68.
27. Mittal V., Akhtar T., and Matsko N. Macromolecular Materials and Engineering. 2015, *300*, 423-435.
28. NOVAMONT. *Copoliéster alifático/aromático biodegradable (AAPE)*. 2010; Available from: http://patentados.com/invento/poliesteres-alifaticos-aromaticos-biodegradables.html.
29. Ferri J.M., Samper M.D., García-Sanoguera D., Reig M.J., Fenollar O., and Balart R. Journal of Materials Science. 2016, *51*, 5356-5366.
30. Lopez-Rodriguez N., Lopez-Arraiza A., Meaurio E., and Sarasua J.R. Polymer Engineering and Science. 2006, *46*, 1299-1308.
31. Lee S. and Lee JW. Korea-Australia Rheology Journal. 2005, *17*, 71-77.
32. Shin B.Y., Jang S.H., and Kim B.S. Polymer Engineering and Science. 2011, *51*, 826-834.
33. Mano J.F., Koniarova D., and Reis R.L. Journal of Materials Science: Materials in Medicine. 2003, *14*, 127-135.
34. Alvarez V.A. and Vázquez A. Polymer Degradation and Stability. 2004, *84*, 13-21.
35. Yu Y., Cheng Y., Ren J., Cao E., Fu X., and Guo W. Journal of Applied Polymer Science. 2015, *132*,
36. Hee-Young Kim S.S.P., Seung-Taik Lim. Colloids and Surfaces B: Biointerfaces. 2014, *126*, 607-620.